

SEISMIC RETROFIT OF RC CIRCULAR COLUMNS USING PREFABRICATED COMPOSITE JACKETING

ABSTRACT: This paper describes experimental and theoretical studies on seismic retrofit of reinforced concrete circular columns with poor lap-splice details using prefabricated composite jacketing. Three 1:2 scale model columns have been tested. One column was tested under the condition of "as built" and two others were tested after being retrofitted using prefabricated composite jacketing. The as-built column suffered brittle failure due to the deterioration of lap-spliced longitudinal reinforcement without developing its flexural capacity or any ductility. The retrofitted columns showed significant improvement in seismic performance. The failed as-built column was retested after being repaired. The repaired column also demonstrated significant improvement in ductility. An analytical model, which takes into consideration the bond-slip deterioration of lap-spliced longitudinal bars, has been developed for seismic assessment and retrofit design.

INTRODUCTION

Several recent destructive earthquakes have indicated that bridges designed and constructed based on older seismic design provisions are vulnerable to catastrophic collapse resulting from the failure of reinforced concrete columns (Priestley 1987; "Loma" 1990; *Preliminary* 1995). Due to the practice of using elastic analyses along with much smaller earthquake forces compared to current design standards, columns in many existing bridges typically have the following potential problems:

1. Undependable flexural capacity due to poor details in longitudinal lap splices
2. Insufficient ductility due to improper transverse confinement
3. Insufficient shear strength
4. Improper details and insufficient strength in the column/footing and column/superstructure joints

There is an urgent need to upgrade existing older bridges to current seismic design standards in regions with high seismicity. Steel jacketing has been proved to be an effective measure to retrofit bridge columns for increased strength and ductility (Chai et al. 1991; Priestley et al. 1994; Xiao et al. 1996). Although steel jacketing has been widely used in practice in California and elsewhere, the society is also looking for other alternatives to improve the retrofitting process for the vast number of existing, structurally deficient bridges both in the United States and throughout the world. One of the key goals is to ease construction.

Advanced composite materials have been recently recognized and applied to bridge retrofit. The general expectations from composite retrofit systems include light weight, high stiffness or strength to weight ratios, etc. Several composite jacketing systems have been developed and validated in laboratory or field conditions. Matsuda et al. (1990) tested a system for bridge pier retrofit using unidirectional carbon fiber sheets wrapped longitudinally and transversely in the potential plastic hinge region or in the region of main bar cutoff. The

carbon fiber sheets were bonded to the concrete surface using epoxy resin. Another composite wrapping system using E-glass fiber, which is much more economical than carbon fiber, has been experimentally studied by Priestley and Seible (1991) and Seible and Priestley (1993). Priestley et al.'s test results on 40% scale bridge piers wrapped with the glass fiber composite jacketing demonstrated significant improvement of seismic performance with increased strength and ductility. Priestley and Seible also developed a full design package for seismic retrofit of existing columns using different retrofit jacketing systems. Saadatmanesh et al. (1994) have proposed a wrapping technique using glass fiber composite straps for column retrofit. Most recently, Seible et al. (1995) have experimentally validated a carbon fiber retrofit system that uses an automated machine to wrap carbon bundles to form a continuous jacket. Successful field construction demonstration is also reported by Seible et al. (1995).

These composite retrofit measures can be categorized as in-situ fabricated jacketing that involves hand or automated machine placement of epoxy saturated glass or carbon fabrics on the surface of existing concrete. An in-situ fabricated jacket can match the shape of the existing column. However, due to the fact of in-situ fabrication, these systems may need special attention to the jobsite quality control and curing of the composite jackets.

A prefabricated composite jacketing system for retrofitting reinforced concrete columns has been recently investigated at the University of Southern California (USC). The retrofit system uses a series of prefabricated E-glass fiber reinforced composite cylindrical shells with slits. When a column is retrofitted, the shells are opened and clamped around the column in sequences with their slits staggered. Adhesive is applied to bond the shells to each other and to the column to form a continuous jacket. The slit for each layer is not butt-bonded and the continuity relies on the subsequent layer. For this reason, the effective layer number is considered as the total number of installed layers subtracting the last layer. The prefabricated jacketing system is expected to have superior constructability in terms of the quality control and the speed of installation. This paper describes the experimental and analytical results from a research program designed to validate the effectiveness of the prefabricated composite jacketing system for improving flexural ductility of bridge columns with lap-spliced longitudinal reinforcement.

EXPERIMENTAL PROGRAM

Model Column Design

Three model columns have been constructed and tested. The model columns were designed based on a 1:2 scale of typical

*Asst. Prof., Dept. of Civ. Engrg., Univ. of Southern California, 3620 S. Vermont Ave., Los Angeles, CA 90089-2531.

*Grad. Res. Asst., Dept. of Civ. Engrg., Univ. of Southern California, 3620 S. Vermont Ave., Los Angeles, CA.

Note. Associate Editor: John B. Man&r. Discussion open until March 1, 1998. To extend the closing date one month, a written request must be filed with the ASCE Manager of Journals. The manuscript for this paper was submitted for review and possible publication on May 24, 1996. This paper is part of *the Journal of Structural Engineering*, Vol. 123, No. 10, October, 1997. ©ASCE, ISSN 0733-9445/97/0010-1357-1364/\$4.00 + \$.50 per page. Paper No. 13339.

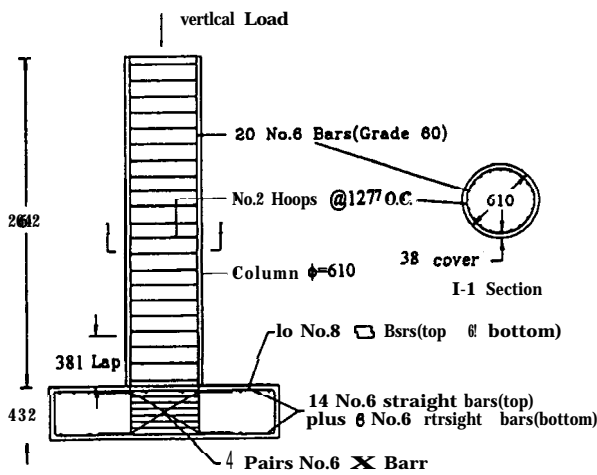


FIG. 1. Model Column Details

1.2 m diameter prototype columns. As shown in Fig. 1, the 2.44 m tall and 0.61 m diameter model columns were reinforced with 20 deformed #6 (nominal diameter = 6/8 in. = 19.1 mm) bars, which constituted a longitudinal steel ratio of 2% of the gross area of column section. The longitudinal steel bars were lap-sliced for a length of 381 mm (15 in.) near the bottom of the column. Round #2 (diameter = 1/4 in. = 6.4 mm) hoops spaced at 127 mm (5 in.) intervals were used as transverse reinforcement.

Due to the difficulties in obtaining Grade 40 (nominal strength = 40 ksi = 276 MPa) steel as specified in the prototype bridge construction, Grade 60 (nominal strength = 60 ksi = 414 MPa) steel was used. Actual yield strength of the Grade 60 steel was 462 MPa (67 ksi) based on tensile test results. Compared to columns reinforced with Grade 40 steel with the same longitudinal steel ratio, a column reinforced with Grade 60 steel subjects to higher demand for shear and bond in the lap-splice region. This implies that the test condition in this program was even more severe than the condition of most existing columns, where Grade 40 steel is common. In addition, the test can also provide an important experimental background for retrofitting older bridges where the designed Grade 40 steel may actually have substantial overstrength. Ready mixed concrete was used throughout. Concrete 28-day cylinder strength was 44.8 MPa (6.5 ksi).

The main experimental parameter was the retrofitting scheme. One model column was tested under the condition of "as-built," while the other two columns were tested after being retrofitted with jacketing. The failed as-built column was repaired by first replacing the loosened concrete with quick-set cement and then installing a 4-layer jacket in the lower

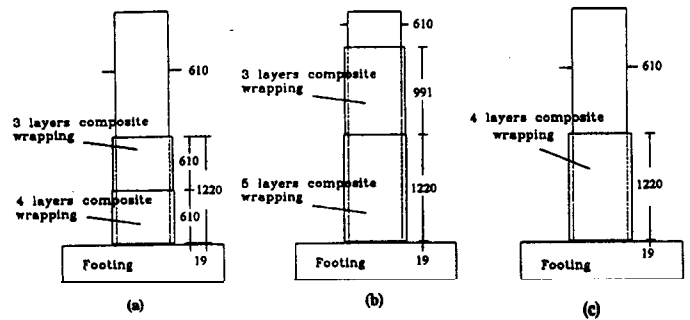


FIG. 2. Retrofit and Repair Details: (a) Retrofit: C2-RT4; (b) Retrofit: C3-RT5; (c) Repair: C4-RP4

half region. The repaired column was then tested to failure. Retrofit and repair details are shown in Fig. 2(a)-(c). The retrofit and repair were applied mainly to the lower portions of the columns to achieve flexural enhancement. However, as shown in Fig. 2(b), one model column was retrofitted for almost full column height with reduced jacket thickness for the upper portion. The upper portion retrofit was mainly for construction demonstration, rather than required by design. The effects due to the upper portion retrofit for this column should be minimal since the moment in the column upper portion was low.

Retrofit Procedure

Each layer of the jackets was prefabricated with unidirectional glass fiber sheets and 2-part epoxy. The layer thickness is approximately 3.2 mm (1/8 in.). The fiber reinforcement is arranged in such way that 90% of the fibers are oriented in the circumferential direction and 10% in the longitudinal direction. The elastic modulus and ultimate strength in the circumferential direction are 48,300 MPa (7,000 ksi) and 552 MPa (80 ksi), respectively, based on the tension tests on flat coupons of the composite jackets. Urethane-based high strength adhesive was used to bond the prefabricated composite shells to form a continuous jacket. Prior to applying the first layer of the composite shells, the column surface was cleaned with a high pressure air gun. Fig. 3 shows the main retrofit procedures for one of the retrofitted test specimens.

Test Method

The test setup was designed to subject the model columns to constant axial load and cyclic horizontal forces in a single curvature condition, as illustrated in Fig. 4. The horizontal force was applied by a + 152 mm (± 6 in.) stroke actuator with the capacity of 1,023 kN (230 kips) in compression and 832

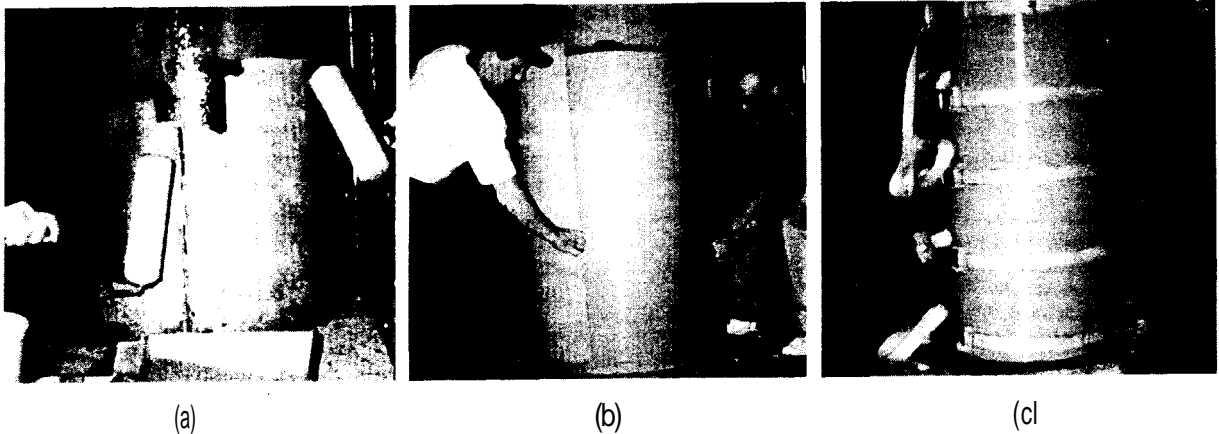


FIG. 3. Installation of Prefabricated Composite Jackets: (a) Applying Adhesive to Column Surface; (b) Installation of Jackets; (c) Curing of Adhesive

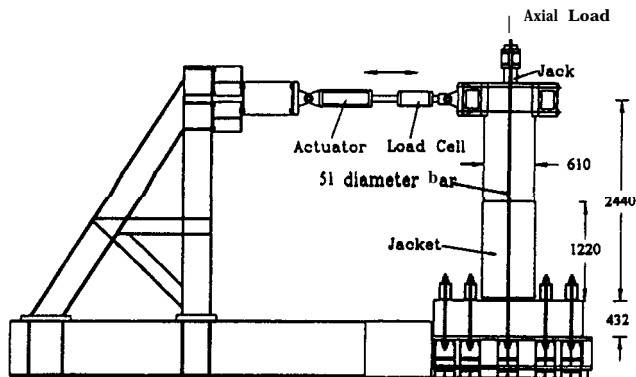


FIG. 4. Test Setup

kN (187 kips) in tension. An axial load of 712 kN (160 kips) was applied to the column by posttensioning two 51 mm (2 in.) diameter high-strength rods with a hydraulic jack at the top of the column. The ratio of the applied axial load to the column axial load capacity was about 5%, which is among the range of typical axial load ratios of columns in multicolumn bent bridges in California. The footing was posttensioned to a reaction beam using eight high strength rods. Instrumentation included all the applied forces and horizontal displacement. Strain gauges were applied to measure the strains of reinforcing steel and composite jacket.

All specimens were subjected to cyclic lateral forces and constant axial load. The lateral loading sequence was controlled by displacement increment based on the reference ductility index. The initial loading cycles were applied corresponding to a peak displacement increment of 2.5 mm (0.1 in.) until the column developed the calculated capacity corresponding to the first yield of longitudinal steel, H_y , for the as-built reference column. Then the reference yield displacement, Δ_y , was determined using the following equation:

$$\Delta_y = \frac{H_y}{H_y} \Delta_1 \quad (1)$$

where \mathbf{A}_1 = average of the measured displacements corresponding to the first yield capacity, H_y , in the push and pull directions; and H_y = calculated ideal flexural capacity of the as-built reference column based on an extreme concrete compressive strain of 0.005 and stress-strain models recommended by Mander et al. (1988). After the column developed the reference first yield capacity, three complete loading cycles were performed at peak displacements corresponding to the reference ductility factors, $\mu_\Delta = 1, 1.5, 2, 3, 4, 6,$ and 8 . The reference ductility factor μ_Δ was defined as the ratio of displacement, \mathbf{A}_1 , to the reference yield displacement, Δ_y . Note that actual loading procedures for different specimens were somewhat different from the standard loading procedure due to the difficulties in displacement control system used in the tests.

EXPERIMENTAL RESULTS

The main experimental observations and results are summarized in this paper. Detailed experimental results can be found elsewhere (Xiao et al. 1995).

Observations

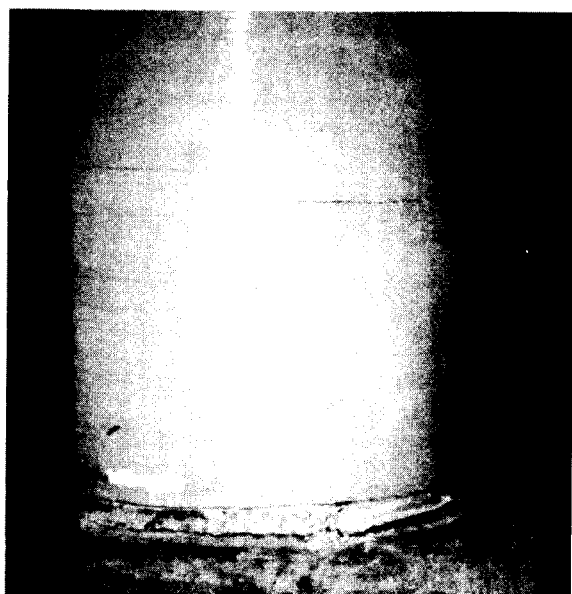
The as-built model column, C1-A, developed an unstable response due to premature lap-splice failure between the longitudinal reinforcement and starter bars. At a displacement of 5 mm (0.2 in.), the first flexural crack was observed at the bottom end of the column. As the displacement increased to 13 mm (0.5 in.), flexural cracks extended into the whole lap-

splice region and then propagated upward. The first vertical crack appeared in the lap-splice region at a displacement of 28 mm (1.1 in.), indicating the initiation of bond slip. After one cycle at a peak displacement of 41 mm (1.6 in.), vertical cracks were fully spread within the lap splice region, indicating the bond-slip failure of lap splices, as shown in Fig. 5(a). The test was terminated when the lateral force capacity dropped to 50% of the maximum capacity at a displacement of 61 mm (2.4 in.).

The retrofitted columns performed in a consistently stable fashion throughout testing. Flexural cracks were observed at the column base where a gap of about 19 mm (0.75 in.) was intentionally provided to prevent the footing from overloading. At the final stages of loading corresponding to a reference displacement ductility factor of 8.0, fine horizontal cracks were observed on the surface of the prefabricated composite jacket, as shown in Fig. 5(b). This was expected because of the smaller fiber content in the longitudinal direction. The repaired column C4-RP4 also exhibited improved performance com-



(a)



(b)

FIG. 5. Crack Patterns: (a) As-Built Column C1-A; (b) Retrofitted Column C2-RT4

paring to the as-built column. The maximum circumferential strain of jackets recorded for all retrofitted columns was approximately 0.001-0.0015 at the bottom of the jacket, similar to the effective strain of 0.001 suggested by Priestley and Seible for composite retrofit (1991). No delamination or rupture across the circumferential fibers of the jackets was observed in any testing of the retrofitted or repaired columns.

At large displacements, deterioration of the bond in the lap splices was observed for all the retrofitted and repaired columns as evidenced by the pullout of the starter bars during the opening of the cracks at the base of the columns. This, along with the measured strains, indicated that performance of the retrofitted or repaired columns at large displacements was also influenced by bond deterioration of the lap-spliced longitudinal bars.

Horizontal Force-Displacement Responses

Plots of horizontal force versus displacement obtained from all four tests are shown in Fig. 6(a)-6(d). Calculated capacities corresponding to the first yield of longitudinal steel, H_y , as ideal flexural capacity, H_{fy} , based on the as-built reference column, are also shown in these diagrams by dashed lines.

As-Built Model Column

Fig. 6(a) shows that the as-built model column C1-A developed unstable hysteresis loops and had rapid degradation in load carrying capacity due to the lap-splice failure. The predicted ultimate flexural strength was not achieved. A maximum horizontal force of 231 kN (52 kips), slightly larger than the calculated first yield capacity, was noted in the pull direc-

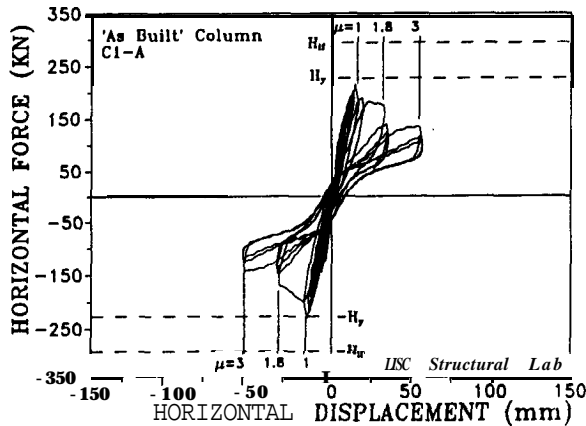
tion corresponding to a displacement of 13 mm (0.5 in.). After the column suffered lap-splice failure, its load carrying capacity stabilized at about 112 kN (25 kips), which was essentially the restoring force due to the applied axial load as the column started rocking about its base.

Retrofitted Model Columns

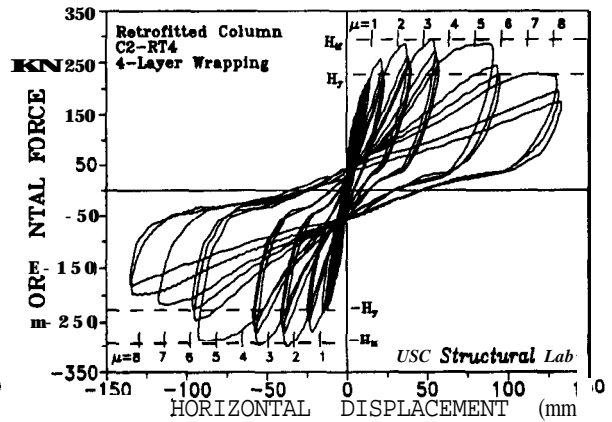
Compared to as-built column C1-A, the two retrofitted columns, C2-RT4 and C3-RT5, exhibited significantly improved seismic performance and demonstrated the effectiveness of the retrofit, as shown in Figs. 6(b) and (c), respectively. The retrofitted column with 4-layer jacketing developed stable hysteretic response up to the first cycle corresponding to the reference ductility factor of about 6.0. The retrofitted column with 5-layer wrapping developed even higher load carrying capacity with a larger ductility factor. Although the load carrying capacities of the retrofitted columns degraded gradually at a ductility factor of 6.0, the columns could develop 70-80% of the ideal flexural strength, even at a displacement ductility factor as large as 8.0 or a drift ratio of about 5.5%. The gradual degradation of the capacity at large displacements was considered due to the bond slip in the lap-spliced longitudinal bars. Such bond slip mechanism can be considered acceptable for seismic retrofit as long as the retrofitted column develops the required load carrying capacity and ductility. A gradual bond slip failure mechanism of the lap-spliced longitudinal bars may be even beneficial since the total failure mode of a column due to the rupture of longitudinal bars can be avoided.

Repaired Model Column

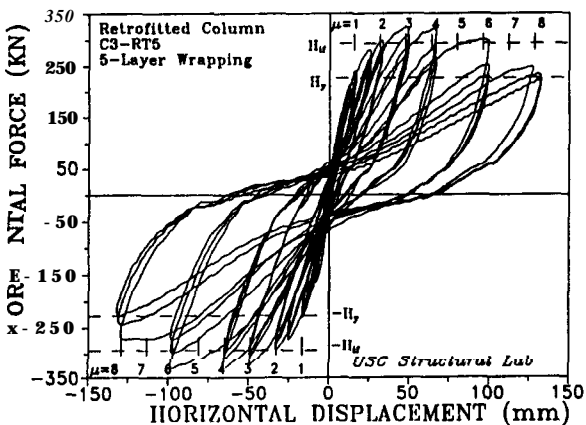
The repaired column C4-RP5 developed a maximum load carrying capacity approximately equal to the first yield



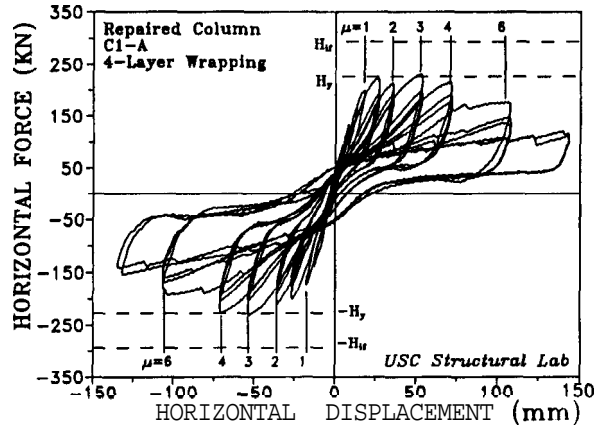
(a)



(b)



(c)



(d)

FIG. 6. Horizontal Force-Displacement Responses: (a) As-Built Column C1-A; (b) Retrofitted Column C2-RT4; (c) Retrofitted Column C3-RT5; (d) Repaired Column C4-RP5

strength calculated on the basis of the virgin section condition, as described in Fig. 6(d). The ductility factors based on the yield displacement defined for as-built column CI-A are shown in Fig. 6(d) as an index indicating the correlation of the displacements of the repaired column and the original as-built column. By comparing the hysteretic responses shown in Figs. 6(a) and (d), it can be seen that the repaired column developed improved behavior than the original as-built column. However, the hysteresis loops of the repaired column are significantly pinched. During loading cycles corresponding to reference ductility factors of 6.0 and 8.0, the hydraulic relief valve in the axial loading system improperly functioned, yielding sudden changes in axial load, which are reflected in the sudden drops in the hysteresis loops beyond $\mu = 4.0$, as shown in Fig. 6(d).

Deterioration of Bond Stresses in Lap Splices

Strain gauges were mounted on the surfaces of the starter bars of the as-built and the retrofitted columns at their critical sections. The stresses in the starter bars at the measured locations can be calculated using the elastoplastic stress-strain relationship and the measured strain data. Average bond stress, $\bar{\tau}$, along the surface of the starter bar can be calculated using the following equation:

$$\bar{\tau} = \frac{f_s d_{lb}}{4L_s} \quad (2)$$

where f_s = stress at the critical section; d_{lb} = diameter of a longitudinal bar; and L_s = length of the lap splice.

In Fig. 7, the average bond stresses in the extreme lap-spliced longitudinal bars of the as-built column CI-A and retrofitted specimen C2-RT4 are plotted against the applied peak displacement ductility factors in the push loading direction. As shown in Fig. 7, the average bond stress for the as-built column deteriorated significantly after the column developed a ductility factor of 1.8. Despite a slight increase in the rebar stress of CI-A at $\mu = 1.8$, the load carrying capacity degraded compared to that at $\mu = 1.0$, as shown in Fig. 6(a). Such a phenomenon probably resulted from the accumulation of the tensile strains of the lap-spliced bars upon cycling. Bond stress in the starter bars of the retrofitted columns was much higher and the degradation was more gradual than in the as-built column, as shown in Fig. 7. In both cases, the bond stress corresponding to the yielding of the steel at critical section, calculated as 5.79 MPa (0.84 ksi), could not be achieved. Despite this, the retrofitted column C2-RT4 was able to develop the first yield capacity, H_y , calculated based on the as-built reference column, as shown in Fig. 6(b). One reason for this is that

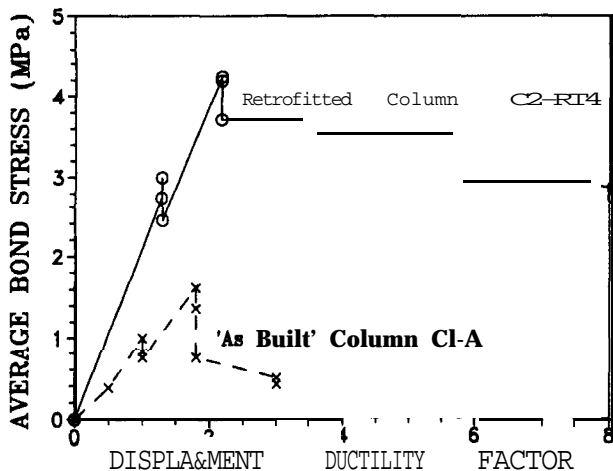


FIG. 7. Degradation of Average Bond Stresses In Lap-Spliced Rebars

the confinement provided by the composite jacket contributed to the capacity increase. Another reason is that in the retrofitted column, the bond deterioration is a gradual process and stress redistribution can be developed after the starter bars slip. From the deformation point of view, the plastification of the hysteresis loops of the columns was mainly resulted from the bond-slip of lap-splice and the nonlinear deformation of the confined concrete, rather than the yielding of longitudinal reinforcement. Thus there is a need to analyze the column performance with taking into consideration the bond deterioration.

ANALYTICAL APPROACH

Analytical Model

In an early study, Xiao et al. (1987) developed a simple analytical model for analyzing the lateral force and displacement performance of short reinforced concrete columns considering both flexural deformation and bond slips in longitudinal bars. A similar model is developed for analyzing the performance of columns with lap splices, as shown in Fig. 8. The analysis is essentially based on the moment curvature analysis with taking into consideration the bond slips of the lap-spliced longitudinal bars.

A hinge is assumed at the bottom of the column, and the upper portion of the column is considered as an elastic beam column. Within the hinge, the curvature is assumed uniform, while a linearly distributed curvature is assumed for the upper portion, as shown in Fig. 8(b). Bond links are assumed for all the lap splices above the hinge length, as shown in Fig. 8(c).

Hinge Length

Priestley and Seible (1991) have suggested the following fixed length of plastic hinges for analyzing inelastic flexural behaviors of reinforced concrete columns with or without jacketing:

$$\text{for as-built columns: } L_p = 0.08h + 0.022d_{lb}f_y \quad (3a)$$

$$\text{for retrofitted columns: } L_p = g + 0.044d_{lb}f_y \quad (3b)$$

where L_p = plastic hinge length; h = height of the column; d_{lb} = diameter of a typical lap-spliced longitudinal bar; f_y = yield strength of the longitudinal reinforcement; and g = gap provided at the bottom of the jacket.

In the proposed approach, the hinge length, L_{ps} , is assumed variable corresponding to the steel stress of the extreme critical tensile bar, f_s . The expression takes the same format of (3a) and (3b) but uses a variable steel stress, f_s , instead of the yield strength f_y .

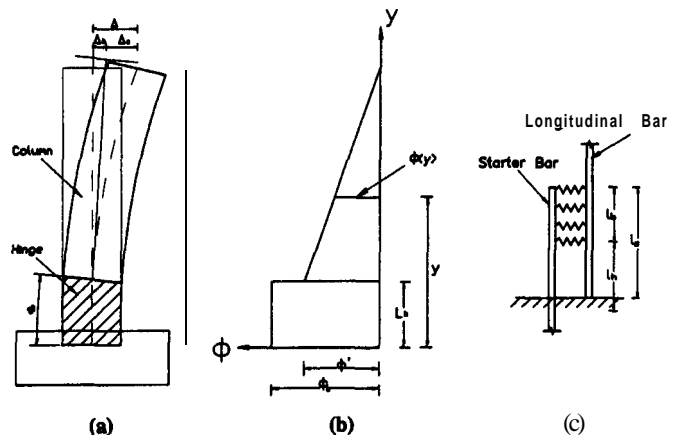


FIG. 8. Analytical Model: (a) Column; (b) Curvature; (c) Bond Links

for as-built columns: $L_h = 0.08h + 0.022d_{lb}f_s$ (4a)

for retrofitted columns: $L_h = g + 0.044d_{lb}f_s$ (4b)

Confined Concrete

Mander et al.'s stress-strain model (1988) is assumed as the constitutive law of the confined concrete. An effective confinement stress provided by the prefabricated jacket is calculated using the following equation:

$$f_i = \frac{2t_j}{D_j - 2t_j} E_f \epsilon_j \tag{5}$$

where f_i = effective confinement stress; D_j and t_j = the diameter and the effective thickness of the jacket; E_f = elastic modulus of the composite in the circumferential direction; and ϵ_j = the effective strain in the jacket. The effective strain of $\epsilon_j = 0.001$ suggested by Priestley and Seible (1991) is used in the analysis.

Bond Links

It is assumed that in the lap-slice region, the stresses in the starter bars are transferred to the longitudinal column bars through a series of bond links, which are distributed throughout a length of L_b given by the following equation:

$$L_b = L_s = 0.022d_{lb}f_s \tag{6}$$

where L_s = length of the lap splices; d_{lb} = diameter of a typical lap-spliced longitudinal bar; and f_s = stress of a longitudinal bar. It should be noted that the length of the bond links defined by (6) is different for rebars at different location in a column section. However, for simplicity, L_b is calculated based on the stress of the extreme tensile bar in the column section. The bond stresses are actually distributed throughout the lap-slice length, L_s , with the peak bond stress occurring between L_s and zero bond stresses at its ends. In this study however, a constant bond stress is essentially used for simplicity. The second term in (6) is provided to minimize the influence due to ignoring the nonlinear distribution of bond stresses within L_s . In future studies, more detailed analysis and calibration of the bond transfer mechanism should be addressed.

The constitutive law for the bond links is expressed by bond stress, τ_b -slip S_b relationship, given by the following equation based on a form of Popovics' equation (1973)

$$\tau_b = \frac{\tau'_{bc} r (S_b / S_{bc})}{r - 1 + (S_b / S_{bc})^r} \tag{7}$$

where τ'_{bc} = peak bond stress between the rebar and confined concrete; S_{bc} = bond slip corresponding to τ'_{bc} ; and r = parameter that defines the shape of the curve expressed by (7) for different transverse confinement. Peak bond stress, τ'_{bc} , can be expressed by the following equation:

$$\tau'_{bc} = \tau'_{b0} + 1.4f_i \tag{8}$$

In (8), the first term, τ'_{b0} , expresses the bond strength for steel bars in plain concrete; the second term expresses the bond strength increment as a consequence of confinement, where f_i is the effective confinement stress calculated using (5) and the coefficient 1.4 is determined based on the shear friction coefficient recommended by AC131 8-89 (Building 1989). On the other hand, following AC1408 Committee report ("State" 1992) the first term of (8) is given by,

$$\tau'_{b0} = 20\sqrt{f'_c/d_{lb}} \leq 5.52 \text{ MPa} \tag{9}$$

Based on trial analyses the upper limit in (9) was ignored.

Parameters S_{bc} and r in (7) are determined using the following empirical equations that were developed for this study us-

ing results of pullout tests on deformed reinforcing bars with different confinement conditions conducted by Giuriani et al. (1991):

$$S_{bc} = S_{b0} \left(1 + \alpha \frac{f_i}{f'_c} \right) \tag{10}$$

where $S_{b0} = 0.25 \text{ mm}$ (0.01 in.); $\alpha = 75.0$; and

$$r = r_0 - k_r \frac{f_i}{f'_c} \tag{11}$$

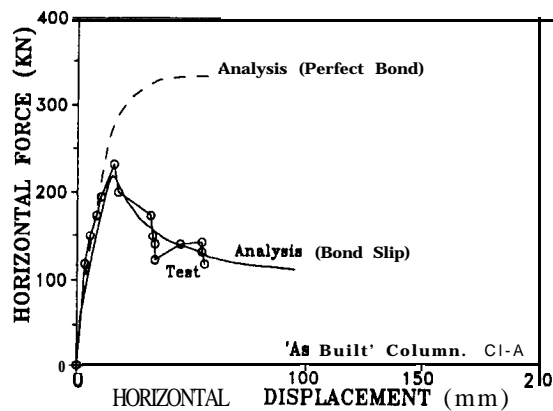
where $r_0 = 2.0$ and $k_r = 13.0$. The maximum value for r should be limited to less than 1.0.

Analytical Procedure

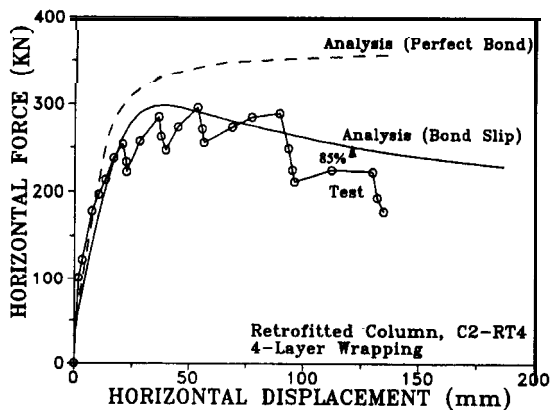
The analytical procedure involves trial and error loops for searching the correct values of the compression zone depth and the bond slip of each individual bar in the critical section, corresponding to each drift displacement increment. The equilibrium condition between bond and tensile force is used as the criteria in finding the bond slip of a lap-sliced bar. The equilibrium condition of the calculated internal axial force and the applied axial load is used as the governing criterion to determine the calculation step of correct neutral axis position in the critical section.

Analytical Results

Analyses have been conducted to simulate the horizontal force-displacement responses of the model columns tested in this study. Figs. 9(a) and (b) show the comparisons of the analytical results and the test results of the horizontal force-displacement envelopes for the as-built model column CI-A



(a)



(b)

FIG. 9. Analytical Results: (a) As-Built Column CI-A; (b) Retrofitted Column C2-RT4

and the retrofitted model column C2-RT4, respectively. Solid lines in Fig. 9 describe the analytical results predicted using the proposed model, with taking into consideration the bond slip of the lap-spliced longitudinal reinforcement. Dashed lines in Fig. 9 show the results of the upper bound analysis in which bond slips of the lap slices are ignored.

As shown in Fig. 9, the analysis based on the proposed model for the lap-sliced column agrees well with the test results and shows reasonable conservatism for both the as-built and the retrofitted conditions. It should be pointed out that the analytical results, which take into consideration the bond-slip for the retrofitted column models, indicate a slightly more rapid degradation after exceeding the peak horizontal load carrying capacity. This is probably due to the conservative nature of the proposed simplified bond-slip law. However, if the ultimate displacement is defined as the lateral displacement corresponding to the point where the horizontal load carrying capacity drops to 85% of the peak capacity, the ductility predicted by the analysis is close to the actual ductility achieved by the test specimens, as shown in Fig. 9(b).

To demonstrate the bond slip mechanisms of the lap-spliced bars, the calculated bond-slip distribution and strain distributions of concrete and longitudinal steel in the hinge region are illustrated in Figs. 10(a) and (b), respectively. The distributions shown in Fig. 10 are corresponded to a calculated column displacement of 51 mm (2.0 in.). As shown in Fig. 10(a), bond slips take place in all the spliced bars in the tension zone, resulting in the relaxation of tensile steel compared to the concrete at the same position, as shown in Fig. 10(b). The consequences are the reduction of the stresses carried by the lap-spliced bars and a slight increase of the concrete compression zone depth. Thus, flexural capacity of the column is reduced

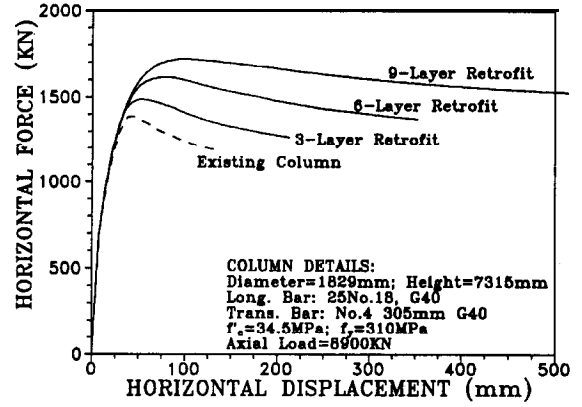
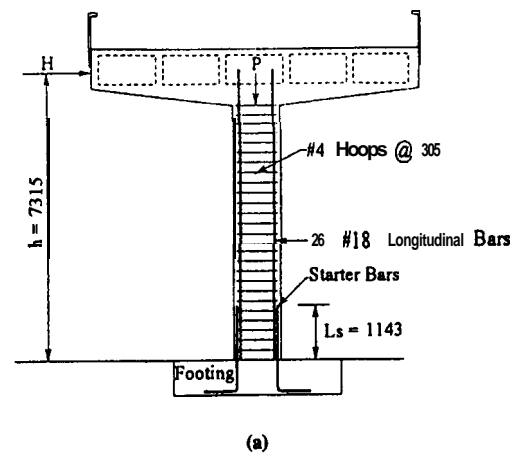


FIG. 11. Design Example: (a) Column; (b) Predicted Responses

compared to the case where perfect bond exists between the bars and concrete.

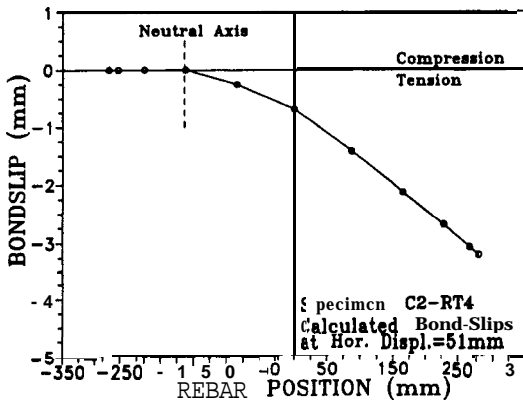
RETROFIT DESIGN RECOMMENDATIONS AND EXAMPLES

The proposed analytical methods can be used as a tool for seismic assessment and retrofit design of existing reinforced concrete bridge columns with lap-spliced longitudinal reinforcement. The procedure involves trial designs of the layer numbers of the prefabricated jackets and prediction of ultimate ductility. If the calculated ductility is less than what is required for retrofit then the number of jacket layers should be increased and the corresponding ductility factor recalculated until the predicted ductility factor exceeds the required value.

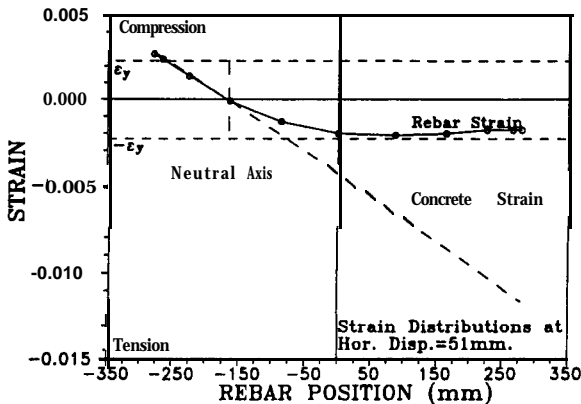
The procedure is demonstrated using a column example shown in Fig. 11(a). The analysis using the proposed model for the existing column indicates that the column is not able to develop its ideal flexural capacity or any ductility; thus retrofit is necessary. A 3-layer wrapping is first assumed for retrofitting the example column. The ductility factor for the 3-layer retrofit is calculated as 5.0, corresponding to the 85% reduction of the load carrying capacity. By doubling the layers to a 6-layer retrofit, a ductility factor of 6.5 is obtained and the design requirement can be satisfied. The number of layers can be further increased to give further design safety. For example, if nine layers of composite jacketing are used, a ductility factor as high as 8.5 can be expected. Horizontal force-displacement responses for all the calculated cases are summarized in Fig. 11(b).

CONCLUSIONS

A prefabricated glass fiber composite jacketing system for seismic retrofit of bridge columns with lap-spliced rebars has



(a)



(b)

FIG. 10. Calculated Bond Slip and Strain Distributions In Lap-Spliced Rebars: (a) Bond Slip; (b) Strains

been experimentally and theoretically studied. Test results of an as-built **model column** indicate that columns with poor lap-splice details are vulnerable to premature brittle failure due to the bond deterioration of the lap-spliced rebars. Such failure pattern can be delayed using the prefabricated composite jacketing, as demonstrated by significantly improved hysteretic responses and increased ductility of the retrofitted model specimens.

Bond slip in lap-spliced rebars can cause a gradual degradation of load carrying capacity of a retrofitted column after the required ductility is developed. Such mechanism may be considered beneficial for retrofit, since a column can be retrofitted with lesser jacket thickness and the total failure mode of the column due to the rupture of longitudinal bars can be avoided.

An analytical approach that takes into consideration the deformation due to the bond slip in lap-spliced longitudinal reinforcement has been developed. Comparison of analytical and test **results** indicates that the analysis provides a rational explanation and prediction to the behavior of columns with lap-spliced longitudinal reinforcement. The proposed method can be used as a useful tool for seismic assessment and retrofit design of columns with lap-spliced rebars as demonstrated by a design example.

ACKNOWLEDGMENTS

The research described in this paper was funded by C. C. Myers Investment, Inc. The prefabricated composite jackets used in the project were manufactured by a joint venture of C. C. Myers, Inc. and NCF Industries, Inc. The writers wish to thank G. R. Martin, professor of USC for his cooperation. Valuable contributions from graduate research assistant Philip Z. Yin of USC in the experimental work are also gratefully appreciated. The comments and conclusions described in this paper are solely those of the writers and do not necessarily reflect the views of the funding agency.

APPENDIX 1. REFERENCES

- Building Code Requirements for Reinforced Concrete and Commentary (ACI318-89/ACI418R-89)*. (1989). American Concrete Institute. Detroit, Mich.
- Chai, Y. H., Priestley, M. J. N., and Seible, F. (1991). "Seismic retrofit of circular bridge columns for enhancing flexural performance." *ACI Struct. J.*, 88(5), 572-584.
- Giuriani, E., Plizzari, G., and Schumm, C. (1991). "Role of stirrups and residual tensile strength of cracked concrete on bond." *J. Struct. Engrg.*, ASCE, 117(1), 1-18.
- "Loma Prieta earthquake reconnaissance report." (1990). *Earthquake Spectra*. Earthquake Engineering Research Institute, Berkeley, Calif.
- Mander, J. B., Priestley, M. J. N., and Park, R. (1988). "Theoretical stress-strain model for confined concrete." *J. Struct. Engrg.*, 114(8), 1827-1849.
- Matsuda, T., Sato, H., Fujiwara, H., and Higashira, N. (1990). "Effect of carbon fiber reinforcement as a strengthening measure for reinforced concrete bridge piers." *Proc., 1st U.S.-Japan Workshop on Seismic Retrofit of Bridges*.
- Popovics, S. (1973). "A numerical approach to the complete stress-strain curves for concrete." *Cement and Concrete Res.*, 3(5), 583-599.

- Preliminary reconnaissance report on the Hyogo-Ken Nambu earthquake of January 17, 1995*. (1995). Earthquake Engineering Research Institute. Berkeley, Calif.
- Priestley, M. J. N. (1987). "Damage of the I-5/3605 separator in the Whinier earthquake of October 1987." *Earthquake Spectra*, 4(2), 389-405.
- Priestley, M. J. N., and Seible, F. (1991). "Seismic assessment and retrofit of bridges." *Struct. Sys. Res. Proj., Rep. No. SSRP-91/103*, University of California at San Diego, Calif.
- Priestley, M. J. N., Seible, F., Xiao, Y., and Verma, R. (1994). "Steel jacket retrofit of squat RC bridge columns for enhanced shear strength. Part 1: Theoretical considerations and test design; and Part 2: Experimental results." *ACI Struct. J.*, 91(4), 394-405; and 91(5), 537-551.
- Saadatmanesh, H., Ehsani, M. R., and Li, M. W. (1994). "Strength and ductility of concrete columns externally reinforced with fiber composite straps." *ACI Struct. J.*, 434.
- Seible, F., and Priestley, M. J. N. (1993). "Retrofit of rectangular flexural columns with composite fiber jackets." *Proc., 2nd Annu. Seismic Res. Workshop*.
- Seible, F., Hegemier, G. A., and Innamorato, D. (1995). "Developments in bridge column jacketing using advance composites." *Proc., Nat. Seismic Conf: on Bridges and Hwy.*, Federal Highway Administration and California Department of Transportation.
- "State-of-the-art report on bond under cyclic loads." (1992). *Report ACI 4082R-92*, American Concrete Institute. Detroit, Mich.
- Xiao, Y., Priestley, M. J. N., and Seible, F. (1996). "Seismic assessment and retrofit of bridge column footings." *ACI Struct. J.*, 93(1), 79-94.
- Xiao, Y., Sakino, K., and Tomii, M. (1987). "Ultimate moment and mechanical behavior of reinforced concrete short circular columns confined in steel tube." *Trans. Japan Concrete Inst.*, 9, Tokyo, Japan, 389-396.
- Xiao, Y., Martin, G., Yin, Z., and Ma, R. (1995). *Bridge column retrofit using snap-tite composite jacketing for improved seismic performance*. Structural Engineering Research Program, University of Southern California. Los Angeles, Calif.

APPENDIX II. NOTATION

The following symbols are used in this paper:

- d_{lb} = diameter of longitudinal bar;
 f_t = transverse confinement stress;
 f_s = steel stress of extreme critical tensile bar;
 f_y = steel yield strength;
 f_c^i = concrete strength;
 g = gap provided at bottom of jacket;
 H_y = ideal flexural capacity for as-built reference column;
 H_y = first yield capacity for as-built reference column;
 L_b = bond link length;
 L_h = variable length of hinge;
 L_p = length of plastic hinge;
 L_s = lap-splice length;
 r = shape parameter for bond stress-strain curve;
 S_b = bond slip;
 S_{bc} = bond slip corresponding to τ'_{bc} ;
 A = average of measured displacements corresponding to H_y ;
 Δ_y = reference yield displacement;
 μ_{Δ} = reference displacement ductility factor;
 τ_b = bond stress;
 τ'_{bc} = bond strength for steel bars in plain concrete;
 τ_{bc} = peak bond stress between rebar and confined concrete; and
 $\bar{\tau}$ = average bond stress along surface of starter bar.